 

# Atomic Radii for Depicting Atoms in a Molecule: Cu in Inert Gas Matrix

**Takatoshi Naka,[1] Yasuyo Hatano,[1] Shigeyoshi Yamamoto,[2] Takeshi Noro,[3] and Hiroshi Tatewaki*[4]**

[1]School of Information Science and Technology, Chukyo University, Toyota 470-0393

[2]School of International Liberal Studies, Chukyo University, Nagoya 466-8666

[3]Division of Chemistry, Graduate School of Science, Hokkaido University, Sapporo 060-0810

[4]Graduate School of Natural Sciences, Nagoya City University, Nagoya 467-8501

Received March 4, 2010; E-mail: htatewak@nsc.nagoya-cu.ac.jp

The effective atomic radius imaging the atoms in an equilibrium molecular structure is discussed for He, Ne, Ar, Kr, and Xe, based on the electrostatic field calculated with the Hartree–Fock and configuration interaction singles and doubles methods, both with and without the Douglas–Kroll–Hess relativistic transformation. The effective atomic radius $r$ is defined as a distance from the nucleus at which the magnitude of the electric field is that in He at one half of the equilibrium bond length of $He_2$. The resulting radii are ca. 20% larger than Bondi's radii, which are conventionally recognized as the van der Waals radii. Valence radii and inner core radii are also defined and discussed.

This work seeks the appropriate atomic size (radius) for imaging the charge distribution when atoms are placed at the equilibrium position of chemical substances. Sometimes it is important to have on image in order to guide subsequent investigations on the molecule.

Three kinds of radius of an atom are useful in considering the atomic charge distribution.

1) The radius at which the atom starts to interact with other atoms, which is called below the effective atomic radius ($r_{ear}$).

2) The radius corresponds to the valence region, including the maximum of the valence charge distribution and a large proportion (around 60%) of the valence electrons, which will be called the valence radius ($r_{val}$).

3) The radius where the electrons of the other atoms hardly encroach, which will be called the core radius ($r_{core}$).

The van der Waals radius[1] is commonly taken as the effective atomic radius, and the valence radius defined by Bragg[2] and Slater[3] is adequate as a standard for the valence radius. These two radii were based on models that constructed crystals out of spheres, in which the bonding atoms approximately touched; the observed intra atomic distance in a crystal between two atoms which form a bond can be written as the sum of the atomic radii of the two atoms. The characteristics of the crystals constrain the characteristics of the radii. The valence radii are close to the values which give the maximum of the valence charge distribution of the gaseous atoms or give the mean distance of $r$, which have been systematically computed with the minimal basis sets.[4] Similar to the valence radius, Yang and Davidson[5] gave a boundary radius which is obtained by an approximate potential being equal to the ionization potential. Before this study we believed that the van der Waals radius (vdw-radius) is adequate to describe the size of the atom, and we next summarize previous investigations of the vdw-radius.

vdw-radii were first determined by Pauling[1] for H and for elements belonging to groups 14, 15, 16, and 17, using structural data for various chemical complexes. Bondi[6] refined these and added the radii for the transition-metal atoms of groups 10, 11, and 12. His values are widely accepted as a standard. Politzer and co-workers[7] considered the atomic valence radii to be the radius at which the electrostatic potential is equal to the chemical potential $\mu$. They used the Thomas–Fermi–Dirac approximation. Extending this work, Deb and co-workers[8] examined physical quantities including the vdw-radii. Recently, Mantina and co-workers[9] determined vdw-radii using ab initio CI calculations with and without relativistic effects approximated by the Douglas–Kroll–Hess (DK) transformation.[10,11] They gave *consistent* vdw-radii for all the elements belonging to the main groups, 1, 2, 13, 14, 15, 16, 17, and 18. However, we find below that the vdw-radius of some atoms given by Bondi is not adequate as a measure of their atomic size.

So far the vdw-radii depend on the solids or molecules used for their determination. We found, however, that for elements in groups 1, 10, 11, and 12 the vdw-radius is approximately equal to or smaller than the mean value $r$ ($\langle r \rangle$) of the outermost shell, so that the vdw-radius above is not appropriate to specify the atomic size. For example, the vdw-radius calculated for Li is 1.81 Å, whereas $\langle r \rangle_{2s} = 2.05$ Å, and the vdw-radius of Cu is 1.4 Å while $\langle r \rangle_{4s} = 1.73$ Å. These inadequacies emerge because of the use of the data from the bulk solid state.

In this paper we aim to determine the effective atomic radius from the electric field calculated for individual atoms. For the valence radius we adopted the mean value of $r$ ($\langle r \rangle$) as suggested by Slater.[3] We calculated the core radius, defined as the radius of a sphere containing 98% of the core electrons. Section 2 sets out the method of calculation. Section 3 gives the effective atomic radii, valence radii, and core radii for the inert gas atoms He, Ne, Ar, Kr, and Xe calculated with and without relativistic effects given by the Douglas–Kroll–Hess transformation.[10,11] Section 4 presents figures for the inert gas

Published on the web June 24, 2010; doi:10.1246/bcsj.20100060

matrices and for Cu in the inert gas matrices drawn using the effective atomic radii ($r_{ear}$'s). Concluding remarks are set out in Section 5.

## Theoretical

$He_2$ is a typical vdw-molecule, and has the smallest dissociation energy ($D_e$) of the diatomics. There is no convention for determining the effective atomic radius ($r_{ear}$), so we define it as the radius at which the electric field is equal in magnitude to that in the He atom at one half of the equilibrium nuclear distance ($R_e$) of $He_2$. The expectation values of the electric field are calculated using the program GAMESS.[12] The wave functions used to calculate $r_{ear}$ are: nonrelativistic Hartree–Fock (NR-HF), nonrelativistic configuration interaction singles and doubles (NR-CISD), relativistic HF with third-order DK Hamiltonian (DK-HF),[13] and relativistic CISD (DK-CISD) wave functions; in the CI calculations the electrons in the valence $(ns)^2(np)^6$ shells are set to be active. The basis sets used for the respective calculations are the following Gaussian-type functions (GTFs).

a) NR-HF: He (5111),[14] Ne (71111/4111),[15] Ar (74111/71111),[15] Kr (743111/74111/7111),[16] Xe (7433111/743111/7411),[17] where '/' separates the s, p, and d symmetries. Numbers greater than 1 denote the numbers of the primitive GTFs (PGTFs) in a contracted GTF (CGTF).

b) NR-CISD: He (NRHF/211/21/2),[18] Ne (NRHF/211/21/2),[18] Ar (NRHF/11/2),[19] Kr (NRHF/11/2),[20] Xe (NRHF/11/2)[20] where NRHF are given in a) and the others are augmented GTFs for describing electron correlation effects. For example, three p, two d, and one f correlating CGTFs are added to the NRHF basis set for He.

c) DK-HF: He (5111),[21] Ne (71111/4111),[21] Ar (74111/71111),[21] Kr (843111/74111/7111),[21] Xe (8433111/743111/7411).[21]

d) DK-CISD: He (DK-HF/211/21/2),[18] Ne (DK-HF/211/21/2),[18] Ar (DK-HF/11/2),[19] Kr (DK-HF/11/2),[20] Xe (DK-HF/11/2)[21] where DK-HF are given in c).

Here we have used the correlation functions common for the nonrelativistic and relativistic calculations.

We also define the valence radius by the following expression;

$$\langle r\rangle = \frac{\sum_i n_{is}(is|r|is) + \sum_i n_{ip}(ip|r|ip)}{\sum_i n_{is} + \sum_i n_{ip}} \quad (1)$$

where $i$ is a principal quantum number of the valence MO. The numbers $n_{is}$ and $n_{ip}$ are occupation numbers of the $is$ and $ip$ HF or natural orbitals. It will be shown that 56–59% of the valence electrons are inside the sphere defined by $\langle r\rangle$ above.

We define the core radius as the radius of a sphere which includes 98% of the core electrons, where the cores for the Ne, Ar, Kr, and Xe are defined as He-, Ne-, $Zn^{2+}$-, and $Cd^{2+}$-like closed-shells, respectively.

## Results

To calculate the values of $r_{ear}$ we first calculated, for the He atom, the magnitude of the electric field at $R_e$(experimental[22])/2 of $He_2$, using the four kinds of wave function specified in Section 2; the magnitudes of the electric fields are 0.00226, 0.00235, 0.00226, and 0.00235 in au for NR-HF, NR-CISD, DK-HF, and DK-CI, respectively. Next, for Ne, Ar, Kr, and Xe, the distance from the nucleus at which the field is the same as for He is calculated. We thereby calculated the effective atomic radius ($r_{ear}$). The results are set out in Table 1, together with $R_e/2$ for the inert gas diatomics and Bondi's vdw-radii, which were redetermined recently by modern CI calculations.[9]

**Table 1.** Effective Atomic Radii (Å) Calculated according to the Electric Field

| Atom | NR-HF | NR-CISD | DK-HF | DK-CISD | $R_e/2$[a)] | Bondi[b)] |
|---|---|---|---|---|---|---|
| He | 1.48 | 1.48 | 1.48 | 1.48 | 1.48 | 1.40 |
| Ne | 1.68 | 1.69 | 1.68 | 1.69 | 1.58 | 1.54 |
| Ar | 2.21 | 2.21 | 2.21 | 2.21 | 1.88 | 1.88 |
| Kr | 2.42 | 2.41 | 2.41 | 2.41 | 2.02 | 2.02 |
| Xe | 2.69 | 2.68 | 2.67 | 2.66 | 2.18 | 2.16 |

a) See Ref. 21. b) See Ref. 5.

Table 1 shows that the $r_{ear}$ values are 10–20% larger than $R_e/2$ or values of the Bondi radius.[6] The $r_{ear}$ values increase with $Z$. NR-HF and NR-CISD give almost the same effective atomic radii, and likewise for DK-HF and DK-CISD. The NR and DK calculations also give almost identical results, except for Xe for which the differences between the nonrelativistic and relativistic calculations, although small, are obvious; the smaller DK $r_{ear}$ values of Xe than the NR values arise from the relativistic corrections effectively increasing the nuclear charge.

Table 2 shows the numbers of valence electrons (NVE) in the $r_{ear}$-sphere and the ratio of these versus NVE. The NVE in the $r_{ear}$-sphere decreases as the nuclear charge $Z$ increases. To maintain the electric field at the value of He electric field, the NVE in the $r_{ear}$-sphere should decrease, since the increase in the $r_{ear}$ suggests that the electric field due to nuclear attraction weakens.

We now discuss the meaning of the condition imposed to obtain $r_{ear}$. The electric field ($E$) at $r_{ear}$ for the atom $I$ is given by

$$\begin{aligned} E(r_{ear_I}) &= -(Z - \mathrm{NVE}(r_{ear_I}))/{r_{ear_I}}^2 \\ &\approx -\rho(r_{ear_I})\Delta r_I/{r_{ear_I}}^2 \\ &= -{r_{ear_I}}^2|F(r_{ear_I})|^2\Delta r_I/{r_{ear_I}}^2 \\ &= -|F(r_{ear_I})|^2\Delta r_I \end{aligned} \quad (2)$$

where the values of $\mathrm{NVE}(r_{ear_I})$ are given in Table 2 and $(Z - \mathrm{NVE}(r_{ear_I}))$ is equal to the number of electrons outside the sphere defined by $r_{ear}$. In the second line in eq 2, $(Z - \mathrm{NVE}(r_{ear_I}))$ is approximated by the electron density at the surface of the sphere multiplied by the effective thickness $\Delta r_I$. In the third line, $|F(r_{ear_I})|^2$ is the radial density at $r_{ear}$ of atom $I$. Table 3 compares $(Z - \mathrm{NVE}(r_{ear_I}))$ and $\rho(r_{ear_I})$. We see that $(Z - \mathrm{NVE}(r_{ear_I}))$ and $\rho(r_{ear_I})$ for the atoms studied scarcely dependent on the calculational methods. The thickness $\Delta r_I$ is estimated from the values given in Table 3 and is between 0.46 bohrs for He and 0.71 bohrs for Xe. The changes in $\Delta r_I$ are relatively small, indicating that the radial densities $|F(r_{ear_I})|^2$ for the respective atoms $I$ are almost the same. Table 4 gives the values of $|F(r_{ear_I})|^2$ and verifies $|F(r_{ear_I})|^2 \approx |F(r_{ear_{He}})|^2$. It follows that to find the $r$ value of the atom $I$ giving the same electric field as He at $R_e/2$ of $He_2$ is approximately equivalent

**Table 2.** Number of Valence Electrons Contained in the Sphere Having the Effective Atomic Radius $r_{ear}$ (NVE-$r_{ear}$-Sphere)

| | Atom | NR-HF | NR-CISD | DK-HF | DK-CISD |
|---|---|---|---|---|---|
| NVE-$r_{ear}$-sphere | He | 1.982 | 1.981 | 1.982 | 1.982 |
| | Ne | 7.977 | 7.975 | 7.977 | 7.975 |
| | Ar | 7.960 | 7.962 | 7.960 | 7.962 |
| | Kr | 7.953 | 7.951 | 7.953 | 7.951 |
| | Xe | 7.942 | 7.940 | 7.942 | 7.940 |
| NVE-$r_{ear}$-sphere/(NVE/%) | He | 99.12 | 99.08 | 99.12 | 99.08 |
| | Ne | 99.71 | 99.69 | 99.71 | 99.69 |
| | Ar | 99.50 | 99.52 | 99.50 | 99.52 |
| | Kr | 99.41 | 99.39 | 99.41 | 99.39 |
| | Xe | 99.27 | 99.25 | 99.27 | 99.25 |

**Table 3.** $Z - \mathrm{NVE}(r_{ear})$ and $\rho(r_{ear})$ for He, Ne, Ar, Kr, and Xe

| | Atom | NR-HF | NR-CISD | DK-HF | DK-CISD |
|---|---|---|---|---|---|
| $Z - \mathrm{NVE}(r_{ear})$ | He | 0.018 | 0.018 | 0.018 | 0.018 |
| | Ne | 0.023 | 0.025 | 0.023 | 0.025 |
| | Ar | 0.040 | 0.038 | 0.040 | 0.038 |
| | Kr | 0.047 | 0.049 | 0.047 | 0.049 |
| | Xe | 0.058 | 0.060 | 0.058 | 0.060 |
| $\rho(r_{ear})$ | He | 0.040 | 0.041 | 0.040 | 0.041 |
| | Ne | 0.054 | 0.059 | 0.054 | 0.059 |
| | Ar | 0.074 | 0.073 | 0.074 | 0.072 |
| | Kr | 0.082 | 0.084 | 0.082 | 0.084 |
| | Xe | 0.092 | 0.094 | 0.092 | 0.094 |

**Table 4.** The Electron Density $|F|^2$ at $r_{ear}$ for He, Ne, Ar, Kr, and Xe

| Atom | NR-HF | NR-CISD | DK-HF | DK-CISD |
|---|---|---|---|---|
| He | 0.0050 | 0.0052 | 0.0050 | 0.0052 |
| Ne | 0.0054 | 0.0057 | 0.0054 | 0.0057 |
| Ar | 0.0043 | 0.0042 | 0.0043 | 0.0042 |
| Kr | 0.0039 | 0.0040 | 0.0039 | 0.0041 |
| Xe | 0.0036 | 0.0037 | 0.0036 | 0.0037 |

to finding $r$ of the atom $I$ giving the same charge density as $|F(r_{He}$ at $R_e/2$ of $He_2)|^2$.

For the valence radius, we adopt the mean value of $r$ given by eq 1) following Slater.[3] The results are set out in Table 5 together with the number of the electrons contained in the sphere of radius $\langle r \rangle$. Irrespective of the computational method, the numbers of electrons in the sphere specified by $\langle r \rangle$ are almost constant for Ne, Ar, Kr, and Xe. The ratio of these numbers to NVE (2 for He and 8 for others) is almost constant, at 59% (He) to 56% (Xe) for all atoms under consideration.

We finally discuss the core radius. In the CI calculations, the *n*s and *n*p electrons are treated as the valence electrons and the He-, Ne-, $Zn^{2+}$-, and $Cd^{2+}$-like closed-shells are kept frozen for Ne, Ar, Kr, and Xe, respectively. When drawing a sphere defined by the core radius ($r_{core}$), it is natural to consider the He-, Ne-, $Zn^{2+}$-, and $Cd^{2+}$-like shells as core, since they form closed-shells and are therefore difficult for other electrons to penetrate, due to the Pauli exclusion principle. Figure 1 shows the charge distribution for these cores and those of the valence shells. For the core charge distribution we show five values of $r$ by solid circles, which indicate $\langle r \rangle$, and $r_i$ ($i$ = 85, 90, 95, and 98) giving the sphere which contains 85%, 90%, 95%, and 98% of the core electrons. We choose $r$(98%) as $r_{core}$, which gives $\rho_{val} \geq \rho_{core}$ for all atoms under consideration. Values of $r_{core}$ are set out in Table 6 for NR-HF and DK-HF only, since the electron correlation effects among the core electrons are not considered and the core orbitals for NR-CI and DK-CI are the same as those of NR-HF and DK-HF. We see that, for the respective atoms, NR-HF and DK-HF give the same values for $r_{core}$, and the same values for the number of the electrons contained in the sphere defined by $r_{core}$.

**Table 5.** The Mean Distance $r$ ($=\langle r \rangle = r_{val}$) and the Numbers of Electrons Contained in the Sphere of Radius $r_{val}$

| | Atom | NR-HF | NR-CISD | DK-HF | DK-CISD |
|---|---|---|---|---|---|
| Valence radius/Å | He | 0.49 | 0.49 | 0.49 | 0.49 |
| | Ne | 0.50 | 0.50 | 0.50 | 0.50 |
| | Ar | 0.85 | 0.85 | 0.85 | 0.85 |
| | Kr | 0.99 | 0.99 | 0.98 | 0.98 |
| | Xe | 1.19 | 1.19 | 1.17 | 1.17 |
| Number of valence electrons contained in the $r_{val}$ sphere | He | 1.17 | 1.17 | 1.17 | 1.17 |
| | Ne | 4.70 | 4.72 | 4.70 | 4.72 |
| | Ar | 4.58 | 4.57 | 4.58 | 4.57 |
| | Kr | 4.56 | 4.56 | 4.56 | 4.56 |
| | Xe | 4.50 | 4.50 | 4.51 | 4.51 |

**Charge Distribution Given by the Effective Atomic Radii.**

In this section we look at the charge distribution of the Cu metal in the inert gas matrix. We also consider the Cu atom in the Ne and Ar matrices. The Cu atom is taken to be located at the substitutional site or the interstitial site. We placed Cu at the hexagonal substitutional site,[23] and considered the nearest Ne or Ar atoms. There have been many investigations, since 1960 and the literature is summarized in the review of Almond and Downs.[24]

Using the MOOTIC program[25] developed by the present authors, we give in Figure 2a the (2s + 2p) charge distribution of the Ne matrix taking the hexagonal closed pack (hcp)

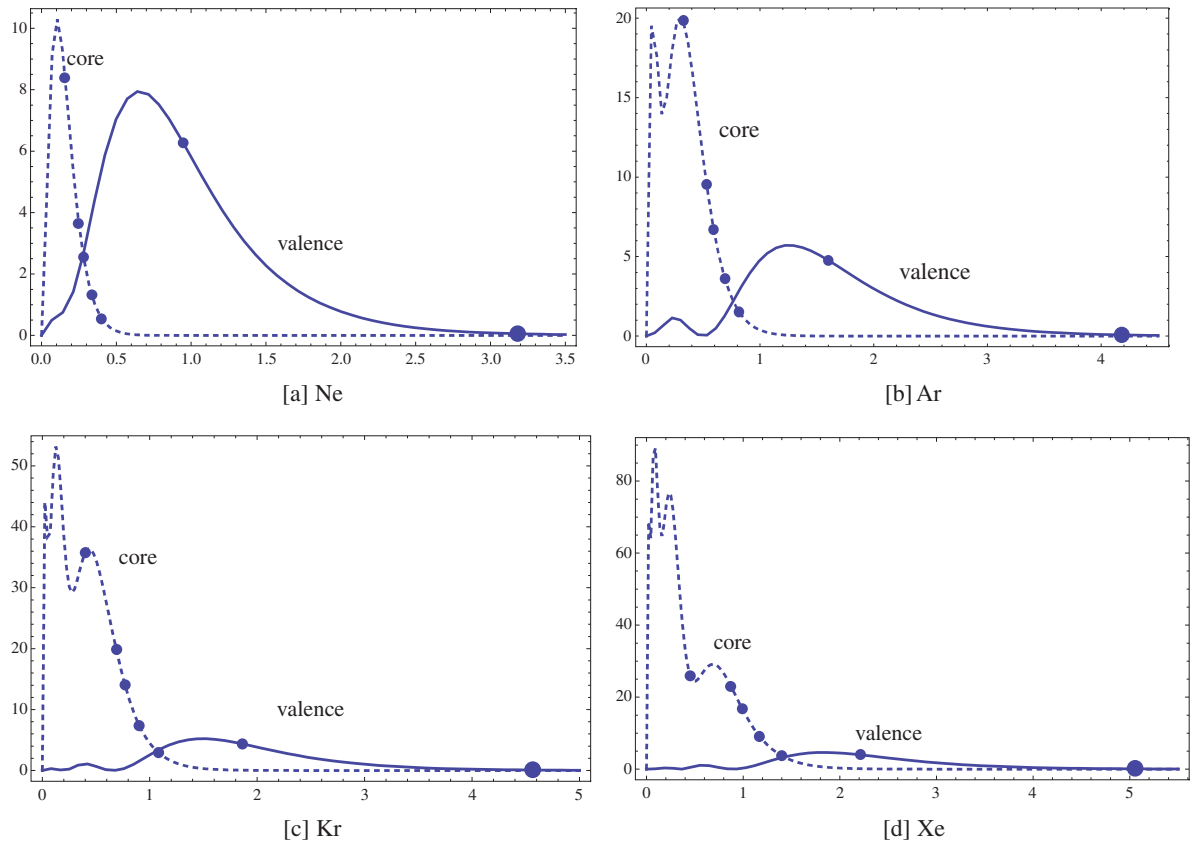


**Figure 1.** Radial charge distribution $\rho(r)$ for the core and valence orbitals. The five solid circles on the core electron distribution indicate $\langle r \rangle$ and the four radii of the spheres containing 85%, 90%, 95%, and 98% of the valence electrons. The two solid circles on the valence shells show $\langle r \rangle$ and the effective atomic radius ($r_{ear}$). The vertical axis gives the charge distribution $r^2|F(r)|^2$, and the horizontal axis is the distance from the nucleus in bohrs; [a] Ne, [b] Ar, [c] Kr, [d] Xe.

**Table 6.** Values of $r_{core}$ and the Numbers of Electrons in the Sphere of Radius $r_{core}$

| Atom | Core radius/Å | | Number of electrons in the $r_{core}$ sphere | |
|---|---|---|---|---|
| | NR-HF | DK-HF | NR-HF | DK-HF |
| Ne | 0.21 | 0.21 | 1.96 | 1.96 |
| Ar | 0.43 | 0.43 | 9.80 | 9.80 |
| Kr | 0.57 | 0.57 | 27.44 | 27.44 |
| Xe | 0.74 | 0.74 | 45.08 | 45.08 |

structure. The matrix is composed of (3,7,3) Ne atoms, where the numbers in parentheses denote the number of atoms held in the first, second, and third planes. We used DK-HF[21] for the charge distribution calculations. The lattice constants are $a = 3.155$ Å and $c = 5.152$ Å, which are calculated from the fcc lattice constant of 4.462 Å.[26] The distance between two adjacent atoms is the same as the lattice constant $a = 3.155$ Å. Since the $r_{ear}$ value of the Ne atom is approximately 1.68 Å, which is close to one half of the lattice constant $a$, the overlaps among the Ne charge distributions are small (Figure 2a). In Figure 2b we give the charge distribution of the Ne matrix + Cu, where the central Ne is replaced by Cu. In the system of the Ne matrix + Cu it is important to consider the overlaps between the Cu 4s and Ne 2s and 2p orbitals, so that we treated only the Cu 4s in determining $r_{ear}$, rather than (4s + 3d). The $r_{ear}$ value calculated for Cu is 2.926 Å, which is 2.1 times larger than the vdw-radius (1.4 Å) given by Bondi.[6] The Cu radius (2.926 Å) is slightly smaller than the lattice constant ($a = 3.155$ Å). The charge distribution of the cage atoms largely covers the Cu 4s region (Figure 2b), showing that the matrix significantly perturbs the Cu atom.

Figure 3a shows the (3s + 3p) charge distribution of the Ar matrix, which also has the hcp structure. We used the DK-HF MO set for Ar from the Ref. 20. The lattice constants $a$ and $c$ are calculated to be 3.759 and 6.138 Å, and are obtained from the fcc lattice constant of 5.316 Å.[26] The $r_{ear}$ value of the Ar atom is 2.21 Å, which is well over one half of the lattice constant $a$. Consequently, a larger overlap of the charge distribution between the two adjacent atoms is observed than that of the Ne matrix (Figure 3a). In Figure 3b, the Cu atom is located at the center of the Ar matrix. Almost all of Cu distribution is covered by the Ar charge distribution.

To see the overlaps between Cu and the matrix more clearly, we give the charge density on the plane that including six inert gas atoms and the Cu atom in Figure 4. The light-red, red, and deep-red colors respectively specify spheres with $r_{ear}$, $r_{val}$, and $r_{core}$ of the inert gas, and the light-blue, blue, and deep-blue colors respectively specify those of Cu. We see that the Cu 4s charge distribution penetrates into the Ne valence region more than into the Ar valence region, indicating that in turn Cu is perturbed more in the Ne matrix than in the Ar matrix.

[a] Ne matrix

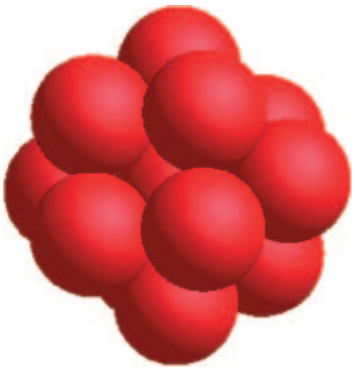

[b] Ne matrix + Cu

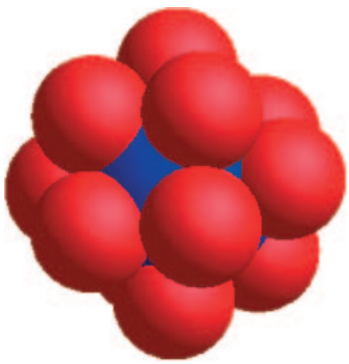

**Figure 2.** [a] Charge distribution of the Ne matrix calculated with DK-HF,[21] 30 bohrs along a side. [b] Charge distribution of the Ne matrix + Cu at the center of the Ne matrix, calculated with DK-HF,[21] 30 bohrs along a side.

[a] Ar matrix

[b] Ar matrix + Cu

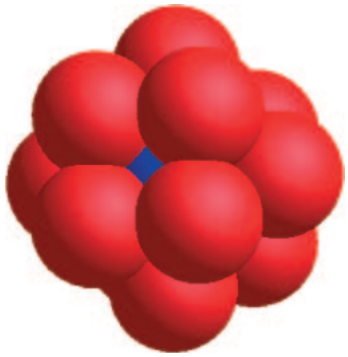

**Figure 3.** [a] Charge distribution of the Ar matrix calculated with DK-HF,[21] 30 bohrs along a side. [b] Charge distribution of the Ar matrix + Cu at the center of the Ar matrix, calculated with DK-HF,[21] 30 bohrs along a side.

We shall shortly see the effect of the matrix atoms on electronic excitations from Cu $(3d)^{10}(4s)^1\ ^2S_{1/2}$ to Cu $(3d)^{10}(4p)^1\ ^2P_{1/2}$ and $(3d)^{10}(4p)^1\ ^2P_{3/2}$. From Figures 2b, 3b, and 4, the excitation energies $(4s)^1\ ^2S_{1/2} \rightarrow (4p)^1\ ^2P_{1/2}$ or $(4p)^1\ ^2P_{3/2}$ in the matrix should be distinct from those of the free gases. A number of experiments have been performed.[27–29] They show that the excitation energies in gaseous Cu are 30535 and 30784 $cm^{-1}$ for $(4p)^1\ ^2P_{1/2}$ and $(4p)^1\ ^2P_{3/2}$,[30] and 32000, 32400, and 33100 $cm^{-1}$ for the Ne matrix and 32700, 33000, and 33500 $cm^{-1}$ for the Ar matrix.[29] The larger valence charge distribution overlap in the Ne matrix + Cu system may lead to greater repulsion of Cu than in the Ar matrix + Cu, inducing greater destabilization of Cu among Ne's than among Ar's and leading to the smaller excitation energies of $(4s)^1\ ^2S_{1/2} \rightarrow (4p)^1$.

We consider one further example. The spin Hamiltonian of Cu in the matrix in a magnetic field $H$[31] is given by

$$\mathrm{H} = g\beta H\cdot\mathrm{S} + A\mathrm{I}\cdot\mathrm{S} \qquad (3)$$

where S and I are the electron and nuclear spin operators of the atom. The $g$ value is approximately 1.999, which is very close to the free spin value of 2.0023.[31] The hyperfine constant $A$ is proportional to the lone pair electron density ($|\Phi(0)|^2$) at the nucleus, where $\Phi$ is composed mainly of Cu 4s and partly of the matrix $n$s and $n$p atomic orbitals. The observed constant $A$'s of Cu in the Ne (6000 MHz) and Ar (6151 MHz) matrices differ markedly from that of the free Cu atom (5867 MHz).[31] Matrix $A$ values larger than the atomic value suggest that electron repulsion between the Cu atom and the matrix causes the Cu electrons to be confined in the region near to Cu nucleus. The greater overlap of Cu with the matrix atoms in the Ne matrix than in the Ar matrix (Figure 4) implies that the weight of Cu 4s in $\Phi$ in the Ne matrix is less than that in the Ar matrix, which in turn causes $|\Phi(0)|^2$ to be smaller in the Ne matrix.

## Conclusion

We have investigated the atomic radius, in order to depict the atomic charge distribution based about the equilibrium position of chemical substances. To this end we calculated the effective atomic radius ($r_{ear}$) at which the electric field has the same magnitude as that of He at $R_e/2$ in $He_2$. We looked at values of $r_{ear}$ calculated with the electrostatic potential given by non-relativistic Hartree–Fock calculations (NR-HF), NR configuration interaction singles and doubles (NR-CISD), and HF with Douglas–Kroll–Hess transformation (DK-HF) and DK-CISD. Irrespective of the calculational scheme, the calculated $r_{ear}$ values for the respective atoms are the same, to high accuracy. The resulting effective atomic radii are 20% larger than Bondi's vdw-radii for the inert gas atoms, and 2.1 times larger for Cu. As examples, we gave the charge distribution of the inert gas matrices. Using the effective atomic radii, we displayed the charge distribution of the constituent atoms of

[a] Ne matrix + Cu

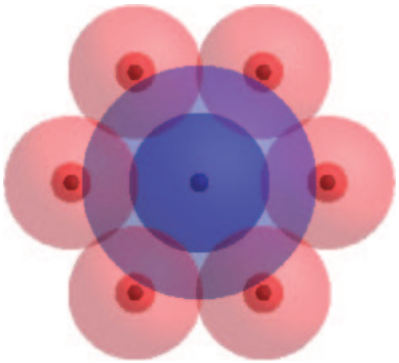

[b] Ar matrix + Cu

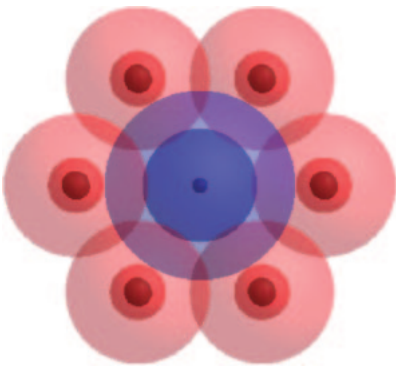

**Figure 4.** [a] Charge distribution of the Ne matrix + Cu on the plane that includes the six Ne and Cu atoms. The light-red, red, and deep-red colors respectively specify the spheres with $r_{ear} = 3.180$ bohrs, $\langle r \rangle = 0.946$ bohrs, and $r_{core} = 0.402$ bohrs for Ne, and the light-blue, blue, and deep-blue colors respectively specify the spheres with $r_{ear} = 5.530$ bohrs, $\langle r \rangle_{4s} = 3.269$ bohrs, and $r_{core} = 0.446$ bohrs for Cu; 30 bohrs along a side. [b] Charge distribution of the Ar matrix + Cu on the plane that includes the six Ar and Cu atoms. The light-red, red, and deep-red colors respectively specify the spheres with $r_{ear} = 4.180$ bohrs, $\langle r \rangle = 1.601$ bohrs, and $r_{core} = 0.815$ bohrs for Ar, and the light-blue, blue, and deep-blue colors respectively specify the spheres with $r_{ear} = 5.530$ bohrs, $\langle r \rangle_{4s} = 3.269$ bohrs, and $r_{core} = 0.446$ bohrs for Cu; 30 bohrs along a side.

these matrices. The charge distribution of the Cu atoms in the Ne and Ar matrices are also shown, and are discussed in line with some spectroscopic results. The investigation on all the atoms from H to Xe is in progress.

## References


1 L. Pauling, *The Nature of the Chemical Bond*, 3rd ed., Cornell University Press, Ithaca, New York, **1960**.

2 W. L. Bragg, *Philos. Mag.* **1920**, *40*, 169.

3 J. C. Slater, *J. Chem. Phys.* **1964**, *41*, 3199.

4 E. Clementi, D. L. Raimondi, W. P. Reinhardt, *J. Chem. Phys.* **1967**, *47*, 1300.

5 Z.-Z. Yang, E. R. Davidson, *Int. J. Quantum Chem.* **1997**, *62*, 47.

6 A. Bondi, *J. Phys. Chem.* **1964**, *68*, 441.

7 P. Politzer, R. G. Parr, D. R. Murphy, *J. Chem. Phys.* **1983**, *79*, 3859.

8 B. M. Deb, R. Singh, N. Sukumar, *J. Mol. Struct.* **1992**, *259*, 121.

9 M. Mantina, A. C. Chamberlin, R. Valero, C. J. Cramer, D. G. Truhlar, *J. Phys. Chem. A* **2009**, *113*, 5806.

10 M. Douglas, N. M. Kroll, *Ann. Phys.* **1974**, *82*, 89.

11 B. A. Hess, *Phys. Rev. A* **1986**, *33*, 3742.

12 *GAMESS, Version 10*, November **2004**; M. W. Schmidt, K. K. Baldridge, J. A. Boatz, S. T. Elbert, M. S. Gordon, J. H. Jensen, S. Koseki, N. Matsunaga, K. A. Nguyen, S. Su, T. L. Windus, M. Dupuis, J. A. Montgomery, Jr., *J. Comput. Chem.* **1993**, *14*, 1347.

13 T. Nakajima, K. Hirao, *Chem. Phys. Lett.* **2000**, *329*, 511.

14 H. Moriyama, private communication.

15 H. Tatewaki, T. Koga, *J. Chem. Phys.* **1996**, *104*, 8493.

16 T. Koga, H. Tatewaki, H. Matsuyama, Y. Satoh, *Theor. Chem. Acc.* **1999**, *102*, 105.

17 T. Koga, S. Yamamoto, T. Shimazaki, H. Tatewaki, *Theor. Chem. Acc.* **2002**, *108*, 41.

18 T. Noro, M. Sekiya, T. Koga, *Theor. Chem. Acc.* **1997**, *98*, 25.

19 M. Sekiya, T. Noro, T. Koga, H. Matsuyama, *THEOCHEM* **1998**, *451*, 51.

20 M. Sekiya, T. Noro, Y. Osanai, T. Koga, *Theor. Chem. Acc.* **2001**, *106*, 297.

21 T. Noro, M. Sekiya, T. Koga, *Chem. Phys. Lett.*, to be submitted.

22 K. P. Hubner, G. Herzberg, *Molecular Spectra and Molecular Structure IV. Constants of Diatomic Molecules*, Van Nostrand Reinhold, New York, **1978**.

23 M. G. Ruffolo, S. Ossicini, F. Forstmann, *J. Chem. Phys.* **1985**, *82*, 3988.

24 M. J. Almond, A. J. Downs, *Spectroscopy of Matrix Isolation Species* in *Advances in Spectroscopy*, ed. by R. J. H. Clark, R. E. Hester, John Wiley & Sons, Chichester, **1988**.

25 MOOTIC (Molecular Orbital Observation Tool with Iso-surface and Cloud): T. Naka, Y. Hatano, S. Yamamoto, H. Tatewaki, M. Endo, M. Yamada, S. Miyazaki, *IEICE Technical Report* **2008**, *108*, 101.

26 *Handbook of Chemistry and Physics*, 80th ed., ed. by D. R. Lide, CRC Press, Boca Raton, Florida, **1999–2000**, Section 12.

27 D. M. Kolb, H. H. Rotermund, W. Schrittenlacher, W. Schroeder, *J. Chem. Phys.* **1984**, *80*, 695.

28 M. Moskovits, J. E. Hulse, *J. Chem. Phys.* **1977**, *67*, 4271.

29 S. Armstrong, R. Grinter, J. McCombie, *J. Chem. Soc., Faraday Trans. 2* **1981**, *77*, 123.

30 C. E. Moore, *Atomic Energy Levels, Circular of the National Bureau of Standards No. 467*, **1952**, Vol. II.

31 P. H. Kasai, D. McLeod, *J. Chem. Phys.* **1971**, *55*, 1566.